

Национална конференция с международно участие „ГЕОНАУКИ 2023“
National Conference with International Participation “GEOSCIENCES 2023”

Redistribution of incompatible elements during hydrothermal alteration of pegmatite from the Djurkovo Pb-Zn deposit, Central Rhodopes

Sylvina Georgieva¹, Rossitsa D. Vassileva¹, Valentin Grozdev¹, Georgi Milenkov¹, Jan Cempírek², Radek Škoda², Eliisa Stefanova¹

¹ Geological Institute, Bulgarian Academy of Sciences, Sofia, Bulgaria; E-mails: sylvina@geology.bas.bg; rosivas@geology.bas.bg; valgrozdev@gmail.com; georgimilenkov7@gmail.com; elitsa.s@gmail.com

² Department of Geological Sciences, Masaryk University, Brno, Czech Republic; E-mails: jan.cempirek@gmail.com; rskoda@sci.muni.cz

Преразпределение на несъвместими елементи при хидротермални изменения на пегматити от Pb-Zn находище Джурково, Централни Родопи

Силвина Георгиева¹, Росица Д. Василева¹, Валентин Гроздев¹, Георги Миленков¹, Ян Цемпирек², Радек Шкода², Елиса Стефанова¹

Abstract. Mineralogical and geochemical study was done on weakly deformed, relatively thin pegmatites that intruded the marbles of the Rhodope metamorphic complex in the Djurkovo Pb-Zn deposit, Central Rhodopes. The pegmatites consist mainly of K-feldspar and quartz and contain minor garnet; the pegmatites lack clear zonation except for the preferable crystallization of the garnet in the central parts. The main accessory minerals are ishikawaite, zircon, monazite-(Ce), apatite, and titanite. The textural relationships indicate later hydrothermal alteration of pegmatites which led to the formation of albite, epidote, sericite, chlorite, carbonate, quartz and leucocoxene. The (REE+Y, ACT, Nb, Ta, Ti)-bearing pegmatite minerals (oxides, silicates and phosphates) are partly leached and/or replaced by secondary ones. The newly-formed phases precipitated as anhedral grains along fractures and dissolved zones onto/or close to the primary minerals due to the limited mobility of the incompatible elements in fluids conditioned by pH, ligand activity and temperature.

Keywords: pegmatites, (REE+Y,U,Th)–(Nb,Ta,Ti) oxide minerals, ishikawaite, fergusonite, fersmite.

Introduction

The incompatible elements (IE) such as REE+Y, actinides (ACT; e.g. Th, U), and HFSE (Zr, Nb, Ta, Ti) are typical elements for NYF family pegmatites (Černý, Ecart, 2005). Considerable part of these elements is referred as strategic and belong to the list of the critical raw materials that are crucial for high technology development. Recent studies show significantly elevated contents of IE in pegmatites of

southern Bulgaria. Field investigation in the Djurkovo Pb-Zn deposit revealed that the ore-hosting metamorphic rock sequence in the region is intruded by pegmatite swarm with variable thickness and position relative to the metamorphic fabrics. These pegmatite dykes are often deformed, boudinaged, folded or cut by later faults. Recent studies revealed that hydrothermal alteration strongly affects the primary pegmatite minerals and led to transformation processes especially in the REE accessory miner-

alization (Georgieva et al., 2022; 2023). This study reports new mineralogical data and preliminary geochemical interpretation about the primary and secondary IE minerals from small volume pegmatites intruded into marbles from the Djurkovo Pb-Zn deposit.

Results and discussion

The focus of this study are relatively thin (≤ 20 cm) pegmatite bodies that intruded in marbles; the pegmatites are predominantly concordant to the fabric of the host rock. These dykes are mainly composed of K-feldspars, quartz and minor garnet. Clear zonal mineral distribution was not observed except for garnet which is concentrated in the central parts of the bodies. Late hydrothermal epidote and chlorite are developed along the pegmatite contacts, penetrating inwards the volume of the pegmatites (Fig. 1A–C). The occurrence, mineral association and chemical composition of the observed minerals are listed in Table 1. The quantitatively predominant K-feldspar suffered albitization. The garnet (up to 5 mm) with inclusions of K-feldspar, quartz, and apatite contains high almandine (42.4–49.1 mol.%) and spessartine (39.5–45.3), and low grossular (2.9–8.2), andradite (0.7–3.6) and pyrope (0.1–3.2) components. The chemical composition of the mineral is additionally characterized with incorporation of Y and Sc as well. The crystals are cracked indicating brittle deformation. Some garnet microfractures are filled with late xenotime-(Y), whereas thortveitite with an increased keiviite-(Y) component and fergusonite-(Y) are precipitated close to its crystal rims (Fig. 1L–O). Among the main pegmatite accessory minerals are fluorapatite, zircon, monazite-(Ce), ishikawaite, and titanite (Fig. 1D–O). Fluorapatite is often observed as euhedral crystals arranged in clusters (Fig. 1D). Its chemical composition reveals high F-content with significant incorporation of Y and LREE. Zircon appears as sub- to euhedral reaching mm-sized crystals with high Hf, U, Sc and HREE incorporation. Monazite-(Ce) forms ≤ 600 μm sub- to euhedral crystals often rimmed by late allanite-

(Ce) and epidote (Fig. 1E). BSE images reveal distinct chemical inhomogeneity due to the variation of REE and Th (Fig. 1F). Occasionally, monazite is observed as relic inclusions in secondary formed allanite-(Ce) (Fig. 1J). Ishikawaite occurs as sub- to euhedral mm-sized crystals often replaced on places by late IE mineralization as fersmite, uraninite and thorite (Fig. 1G–I). The chemical composition of the mineral is characterized with high content of U, Y, Sc Th and REE. Due to metamictization SiO_2 is generally intruded (≤ 0.14 wt %). Titanite is rarely observed as preserved anhedral ≤ 600 μm grains often in association with allanite and epidote (Fig. 1K) but most often it is replaced by *leucoxene* and calcite.

The studied pegmatite bodies are considered as part of the host metamorphic frame of one of the largest base metal deposits in the Central Rhodopes and hence the whole rock volume is strongly influenced by late hydrothermal events (pre- and syn-ore-forming). The pegmatites comprise large number of accessory minerals concentrating significant amounts of IE (such as REE+Y, Th, U, Sc, Nb, Ta, *etc.*) – part of them assigned as critical for the modern industry. Despite the activity of the late hydrothermal alteration and metasomatic processes in the Pb-Zn deposit, the present study reveals that the IE remained mostly in the rock volume, although redistributed as newly-formed phases. The main reason for the latter is due to IE restricted mobility, which is highly dependent on the mineralizing conditions. The primary pegmatite minerals (*e.g.*, garnet, ishikawaite, monazite, titanite) affected by transformations are cracked, altered and replaced by secondary ones (xenotime, thortveitite-keiviite-(Y), fergusonite, fersmite, uraninite, thorite). The observation of small-scale hydrothermally altered IE-bearing pegmatites might be a useful tool for tracing the redistributing mechanism of these elements.

Acknowledgements: The study is financially supported by the Bulgarian National Science Fund projects KP-06-N34/4 and ERA-MIN PEGMAT project KP-06-DO02/2.

Fig. 1. A, macrophotograph of the pegmatite intruded in the marble; B, C, occurrence and relationships of the primary and secondary hydrothermal mineralization; D–O, BSE images of occurrence and textural relationships between primary accessory minerals and the secondary ones: D, ishikawaite and aggregation of apatite among K-feldspar and quartz with late developed chlorite, albite and uraninite; E, accessory monazite rimmed by allanite; F, close view of E: REE compositional inhomogeneity in monazite; G–I, different magnification of textural relationships between primary ishikawaite and secondary mineral phases developed on it; J, relics of monazite and allanite, enclosed in epidote with late developed REE-epidote and xenotime; K, allanite, titanite and zircon enclosed in later epidote; L, anhedral grains of xenotime developed on cracks in the garnet; M, N, late thortveitite and fergusonite developed in close proximity to the garnet; O, euhedral zonal thortveitite crystals in chlorite. The zonal pattern is determined by the variation of Y and Sc composition. The brighter rims are rich in keiviite-(Y) component. Abb.: Kfs, K-feldspar; Qz, quartz; Gar, garnet; Ab, albite; Ep, epidote; REE-Ep, REE-epidote; Chl, chlorite; Hem, hematite; Mnz, monazite; Ikw, ishikawaite; Ap, apatite; Aln, allanite; Ttn, titanite; Zrn, zircon; Fsm, fersmite; Xtm, xenotime; Tvt, thortveitite; Kvi-Y, keiviite-(Y); Fgu, fergusonite; Ur, uraninite; Thr, thorite.

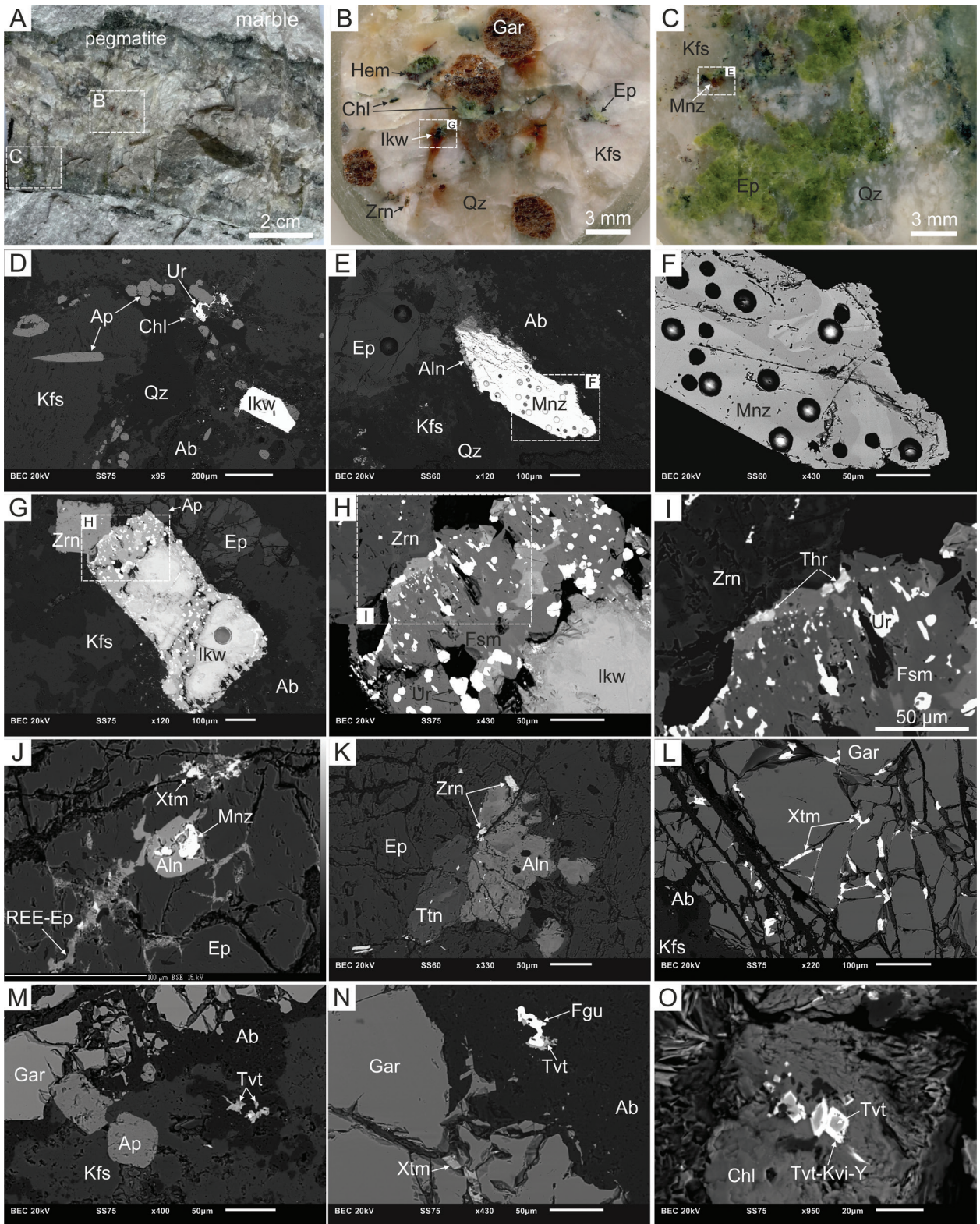


Table 1. Occurrence, mineral association and chemical properties of the minerals

Minerals	Occurrence and mineral association	Crystal chemical composition of representative analyses
		max. values for significant trace element (ppm)
<i>Major</i>		
K-feldspar	massive cm-sized aggregates + quartz, garnet, apatite, zircon, ishikawaite, monazite, later albite, epidote, chlorite, xenotime	$(K_{0.920}Na_{0.109}Ca_{0.002})_{1.030}(Al_{0.986}Fe_{0.001})_{0.987}Si_{3.003}O_8$ Rb (622), Ba (215), Pb (122), Sr (114), Ga (35)
Garnet	euhedral, ≤5 mm + K-feldspar, quartz, later albite, epidote, chlorite, xenotime, thortveitite, fergusonite	$(Fe^{2+}_{1.273}Mn_{1.359}Ca_{0.243}Mg_{0.090}Y_{0.025}Na_{0.010})_3(Al_{1.878}Fe^{3+}_{0.083}Fe^{2+}_{0.007}Sc_{0.012}Ti_{0.008}Sn_{0.001})_{1.999}(Si_{2.993}Al_{0.007})_3O_{12}$ Yb (960), Er (458), Dy (412), Lu (149), P (140), Zn (130), Ho (108), Tm (98), Gd (95), Ga (79), Ge (78), Li (57)
<i>Accessories</i>		
Fluorapatite	sub- to euhedral, ≤200 μm + K-feldspar, garnet, quartz, apatite, ishikawaite, later albite, epidote, chlorite, uraninite	$(Ca_{4.829}Mn_{0.026}Na_{0.009}Fe_{0.006}Ce_{0.004}Nd_{0.004})_{4.878}(P_{2.881}Si_{0.015}O_4)_3(F_{0.745}Cl_{0.036})$ Y (2055), Nd (1138), Ce (1103), Sm (720), Gd (683), Dy (387), La (231), Pr (213), Er (189), Yb (111), Sr (110), Tb (93), Ho (73), Ge (33)
Zircon	Sub- to euhedral, ≤1 mm + K-feldspar, quartz, ishikawaite, allanite, titanite, apatite, later albite, epidote, chlorite, uraninite	$(Zr_{0.928}Hf_{0.044}U_{0.015}Sc_{0.013}Y_{0.001}Er_{0.001}Yb_{0.001}Th_{0.001}Fe_{0.001})_{1.005}Si_{0.993}O_4$
Monazite-(Ce)	sub- to euhedral, ≤600 μm + K-feldspar, quartz, later albite, epidote, REE-epidote, allanite, xenotime, chlorite	$(Ca_{0.012}Y_{0.040}La_{0.173}Ce_{0.398}Pr_{0.046}Nd_{0.160}Sm_{0.039}Gd_{0.026}Tb_{0.003}Dy_{0.009}Er_{0.002}Th_{0.056}U_{0.003})_{0.970}(P_{0.974}Si_{0.055})_{1.029}O_4$ Tb (1114), Eu (389), Tm (158), Yb (650), Lu (57), Pb (284)
Ishikawaite	sub- to euhedral, ≤1 mm + K-feldspar, quartz, zircon, apatite, later albite, epidote, fersmite, uraninite, thorite	$[(Y_{0.262}Gd_{0.057}Dy_{0.052}Sm_{0.047}Nd_{0.043}Ce_{0.019}Pr_{0.007}Er_{0.005}Yb_{0.003}Tb_{0.003})_{0.498}U_{0.463}Th_{0.084}Ca_{0.077}Fe_{0.618}Mn_{0.111}Sc_{0.100}Mg_{0.006}Pb_{0.014}]_{1.974}(Nb_{1.874}Ta_{0.053}Ti_{0.049}W_{0.019}Zr_{0.018})_{2.013}O_8$ Sn (2367), Ho (1308), Ba (418), Sr (270), La (253), Tm (245), Ge (243), As (255), Hf (140), Zn (140), Sb (114), Bi (101), Lu (101), Ga (87), Be (37)
Titanite	sub- to euhedral, ≤600 μm + K-feldspar, quartz, allanite, apatite, zircon, later leucoxene, chlorite, calcite, sericite, xenotime, hematite	$Ca_{0.946}(Ti_{0.903}Al_{0.103})_{1.006}Si_{1.047}O_5$
<i>Secondary</i>		
Albite	aggregates in veins and nests among K-feldspar and garnet + quartz, epidote, chlorite, fergusonite, thortveitite	$(Na_{0.935}Ca_{0.027}K_{0.007})_{0.969}(Al_{0.998}Fe_{0.009})_{1.007}Si_{2.997}O_8$ Sr (286), Rb (117), Ga (71), Be (35), Zn (26), Li (20)
Allanite-(Ce)	anhedral, ≤200 μm + monazite, zircon, titanite, late REE-epidote, epidote, chlorite, xenotime	$(Ca_{0.982}Ce_{0.422}La_{0.181}Nd_{0.153}Pr_{0.047}Sm_{0.023}Gd_{0.018}Y_{0.025}Th_{0.020}Mn_{0.168})_{2.040}(Al_{1.363}Fe^{2+}_{0.875}Fe^{3+}_{0.543}Mg_{0.087}Ti_{0.048})_{2.916}(Si_{3.044}O_4)_3(OH)$
Epidote	cm-sized aggregates in veins and nests + allanite, monazite, chlorite, hematite, calcite, sericite	$(Ca_{2.019}Y_{0.002})_{2.022}(Al_{2.070}Fe^{3+}_{0.916}Mn_{0.004})_{2.991}(Si_{2.988}O_4)_3(OH)$ Y (516), Sr (388), Ga (191), Rb (154), U (134), Ce (74), Dy (67), Sn (57), Sc (53), Er (50), Yb (43), Nd (39), Gd (32), La (31)
Xenotime-(Y)	anhedral grains in garnets and epidote ± chlorite	$(Y_{0.748}Dy_{0.072}Yb_{0.038}Er_{0.034}Gd_{0.021}Ho_{0.012}Tb_{0.007}Sm_{0.006}U_{0.005}Tm_{0.005}Lu_{0.005}Nd_{0.002}Sc_{0.012}Fe_{0.021}Mn_{0.018}Ca_{0.004}Pb_{0.003})_{1.015}(P_{0.863}Si_{0.122})_{0.985}O_4$
Thortveitite	anhedral grains ≤20 μm next to garnet + chlorite, fergusonite, albite	$(Sc_{1.423}Y_{0.271}Zr_{0.145}Yb_{0.055}Er_{0.018}Dy_{0.014}Lu_{0.009}Gd_{0.007}Tm_{0.005}Ho_{0.003}Fe_{0.022}Ca_{0.009}Ti_{0.007})_{1.990}(Si_{1.967}Al_{0.044})_{2.010}O_7$
Fergusonite-(Y)	anhedral grains ≤50 μm + garnet, thortveitite, albite	$(Ca_{0.078}Y_{0.623}Dy_{0.051}Yb_{0.051}Er_{0.038}Gd_{0.029}Lu_{0.008}Ho_{0.007}Tm_{0.006}Tb_{0.004}Sm_{0.003}Nd_{0.002}Ce_{0.001}Sc_{0.001}Fe_{0.028}Mn_{0.010}U_{0.020}Pb_{0.001})_{0.967}(Nb_{0.949}W_{0.044}Ta_{0.011}Ti_{0.007}Zr_{0.001})_{1.013}O_4$
Fersmite	μm-sized aggregates in nest and veinlets in ishikawaite + uraninite, thorite	$(Ca_{0.961}Y_{0.048}Th_{0.009}U_{0.009}Sc_{0.006}Dy_{0.006}Gd_{0.005}Yb_{0.003}Er_{0.002}Tm_{0.002}Lu_{0.001}La_{0.001}Nd_{0.001}Tb_{0.001}Ho_{0.001}Fe_{0.013}Mn_{0.003})_{1.071}(Nb_{1.819}Ti_{0.054}Ta_{0.038}Zr_{0.007}W_{0.005})_{1.923}(O,OH)_6$
Uraninite	anhedral grains ≤20 μm in ishikawaite and zircon + fersmite, thorite	$(U_{0.825}Th_{0.107}Y_{0.029}Ca_{0.066}Pb_{0.005}Dy_{0.005}Gd_{0.003}Yb_{0.002}Ce_{0.001}Sm_{0.001}Er_{0.001})_{1.045}O_2$

Note: EPMA analyses were carried out at the Laboratory of Electron Microscopy and Microanalysis, Department of Geological Sciences, Masaryk University, Brno. Trace element composition was determined by LA-ICP-MS at the Geological Institute, Bulgarian Academy of Sciences.

References

- Černý, P., T. S. Ecart. 2005. The classification of granitic pegmatites revisited. – *The Canadian Mineral.*, 43, 2005–2026; <https://doi.org/10.2113/gscanmin.43.6.2005>.
- Georgieva, S., R. D. Vassileva, G. Milenkov. 2022. Mineral association in pegmatites from the Djurkovo Pb-Zn deposit, Central Rhodopes: preliminary results. – *Rev. Bulg. Geol. Soc.*, 83, 3 (Geosciences 2022), 19–22; <https://doi.org/10.52215/rev.bgs.2022.83.3.19>.
- Georgieva, S., R. D. Vassileva, G. Milenkov, J. Cempírek, R. Škoda. 2023. Rare-earth element mineralization in altered pegmatites from the Djurkovo Pb-Zn deposit, Central Rhodopes. – In: *17th SGA Biennial Meeting "Mineral Resources in a Changing World"*, 28th August–1st September 2023, Zurich, 31–34.